energies

MDPI

Article

Study of the Impact of Initial Moisture Content in Oil Impregnated Insulation Paper on Thermal Aging Rate of Condenser Bushing

Youyuan Wang [1], Kun Xiao [1,*], Bijun Chen [1,2] and Yuanlong Li [1]

Received: 19 October 2015; Accepted: 11 December 2015; Published: 18 December 2015
Academic Editor: Issouf Fofana

[1] State Key Laboratory of Power Transmission Equipment & System Security and New Technology, Chongqing University, Chongqing 400044, China; y.wang@cqu.edu.cn (Y.W.); 13883957738@163.com (Y.L.)
[2] State Grid Tianjin Electric Power Supply Company, Tianjin 300457, China; bijunch@126.com
* Correspondence: 20104427@cqu.edu.cn; Tel.: +86-133-6836-5907

Abstract: This paper studied the impact of moisture on the correlated characteristics of the condenser bushings oil-paper insulation system. The oil-impregnated paper samples underwent accelerated thermal aging at 130 °C after preparation at different initial moisture contents (1%, 3%, 5% and 7%). All the samples were extracted periodically for the measurement of the moisture content, the degree of polymerization (DP) and frequency domain dielectric spectroscopy (FDS). Next, the measurement results of samples were compared to the related research results of transformer oil-paper insulation, offering a theoretical basis of the parameter analysis. The obtained results show that the moisture fluctuation amplitude can reflect the different initial moisture contents of insulating paper and the mass ratio of oil and paper has little impact on the moisture content fluctuation pattern in oil-paper but has a great impact on moisture fluctuation amplitude; reduction of DP presents an accelerating trend with the increase of initial moisture content, and the aging rate of test samples is higher under low moisture content but lower under high moisture content compared to the insulation paper in transformers. Two obvious "deceleration zones" appeared in the dielectric spectrum with the decrease of frequency, and not only does the integral value of dielectric dissipation factor (tan δ) reflect the aging degree, but it reflects the moisture content in solid insulation. These types of research in this paper can be applied to evaluate the condition of humidified insulation and the aging state of solid insulation for condenser bushings.

Keywords: oil-impregnated paper; initial moisture content; thermal aging; frequency domain dielectric spectroscopy (FDS); degree of polymerization (DP); dielectric dissipation factor (tan δ)

1. Introduction

Currently, 30% of the cases of main transformer faults are caused by bushing troubles, which is a key threat to the safety of the power grid [1–5]. Most high voltage bushings are condenser bushings. The main types of insulation of condenser bushings are capacitor cores, which are conductive rods wrapped by multi-layer insulation paper and aluminum foils, and the insulation performance of condenser bushings is vulnerable [1,3]. In the core, the aluminum foils are used to make the electric field uniform; however, the edges of aluminum foil are more likely to have discharge compared to the oil-paper insulation in transformers [1]. In addition, without radiators and cooling devices in bushing, it is easy for heat to accumulate around the conductive rod when the bushing is under operation or even lead to an explosion [1]. The failure rate of the other parts of bushings is far less than that of the capacitor core [6]. Thus, the crucial insulation part of capacitive bushing is the internal capacitive core [7].

Statistical data has shown that the main reasons for oil-paper capacitive bushing failures are the following: moistened insulation, manufacturing defect, oil leakage, insulation aging, and the failures caused by moistened insulation is the most common [2,3]. Studies have shown that thermal degradation, hydrolysis and oxidation degradation are the three main predominant factors causing the deterioration of oil-paper insulation [4]. In addition, the moisture absorption ability of insulation paper is much stronger than that of insulation oil [5]; therefore, studying the influence of moisture on the aging characteristics of oil-paper bushing has engineering significance for evaluating the insulation loss caused by moisture.

At present, dielectric spectroscopy in time or frequency domain offers new opportunities for an off-line, insulation condition assessment of high voltage (HV) electric power equipment and its predictive maintenance nondestructively and reliably in the field [8–11]. Dielectric spectroscopy techniques in time and frequency domain can be applied to monitor the condition of oil-impregnated paper condenser bushings [9]. The results researched by Issouf Fofana *et al.* indicate that capacitance ratio and direct current conductivity deduced from the spectroscopic measurements can be used to accurately monitor insulation condition, and both parameters were found to increase with moisture or aging duration [8]. In addition, the poles computed from frequency domain spectroscopy also can assess oil-paper insulation condition [11]. It is mentioned in [12,13] that the dielectric spectroscopy of oil-paper condenser bushing is different from that of oil-paper in transformers at low frequency interval and the characteristics of dielectric spectroscopy at frequency interval 10^{-2}–10^{3} Hz can sensitively reflect the variation of moisture content in condenser bushing. However, the condition of oil-impregnated paper condenser bushings is qualitatively assessed in these research reports. More accurate diagnostic methods are necessary to be researched based on dielectric spectroscopy.

In this article, a 43-day accelerated thermal aging under 130 °C is carried out for samples, referring to the humidified insulation test of transformer oil-paper [14,15]. In addition, the moisture content, degree of polymerization (DP) and dielectric dissipation factor (tan δ) of samples are periodically measured during the aging process. The change rules of these measurements have been analyzed in this article, and the quantitative assessment on the remaining life of oil-paper condenser bushing has also been discussed in this investigation.

2. Preparation for Thermal Aging Test

2.1. Test Sample

The capacitor core of condenser bushing is a conductive rod wound by multi-layer insulation paper and aluminum foils [9]. The construction of capacitor core is shown in Figure 1. It is mentioned in [7] that the main manufacturing steps for a bushing consist of rolling the capacitor core, vacuum drying, assembly and vacuum oil immersion, as shown in Figure 2.

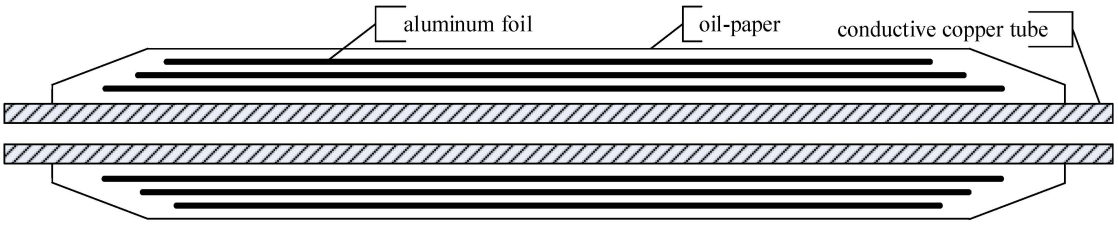

Figure 1. The structure diagram of a condenser core.

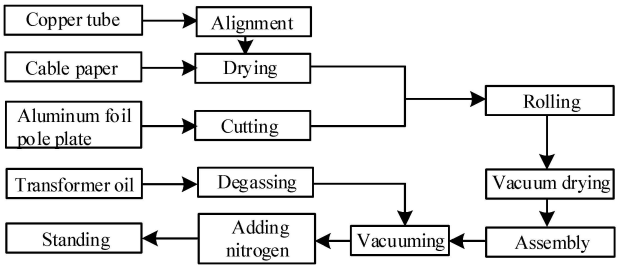

Figure 2. The manufacturing steps of a condenser core [7].

The manufacturing steps are as follows:

(1) Test materials preparation

Insulation paper with 0.12 mm in thickness, aluminum foil with 0.01 mm in thickness, copper tube with 10 mm in outer diameter and 96 mm in length, and #25 Karamay transformer oil (ρ = 0.8846 g/cm^3). The insulation paper is shaped into rectangular paper tape with 96 mm in width, 1390 mm in length and each tape weighs 16.62 g.

(2) Identify the layer number of aluminum foil and the thickness of insulation

In accordance with the insulation requirement of a 10 kV bushing, according to reference [7], the number of layers should be three. The common insulation layer thickness is approximately 1.0–1.2 mm, so a nine-layer cable paper (approximately 1.08 mm) is selected as an insulating layer. Because the designed capacitor core model of bushing is far smaller than that of real bushing, the length of the aluminum foil and insulation paper has little effect on the investigation. The length of the aluminum foil and the width of the copper tube and insulation paper are set to the same value for convenience.

(3) Winding capacitor core

Using the modified winding machine to wind the cable paper tightly around the copper tube, one-layer aluminum foil was wound after winding nine-layer paper. The width of aluminum foil is shown in Table 1 and the length is 96 mm, the same as the paper. After winding the three-layer aluminum foils, wind all the remaining insulating paper and then fix with white gauze. The capacitor core model of bushing is shown in Figure 3.

Table 1. The width of aluminum foil.

The Layer Number	1	2	3
The width of aluminum foil/mm	38.33	45.61	53.09

Figure 3. The capacitor core model of condenser bushing.

2.2. Control of the Initial Moisture Content

The capacitor core models of bushing are divided into four groups (respectively named A, B, C, and D) by four kinds of initial moisture content, and each group has seven models. These models are placed into 28 wide mouth flasks, respectively. Each flask contains a capacitor core model and

an additional 21 pieces of paper. The size of added paper is 85 mm × 695 mm, and the total mass is 116.77 g. Thus, each flask requires 133.39 g insulating paper and 230 mL of dehydrated and degassed #25 transformer oil to ensure that the mass ratio of oil and paper is roughly equal to 1.5. The details of treating process are as follows:

(1) Place the group A unsealed wide mouth flasks in a vacuum drying oven, set the temperature to 90 °C and the vacuum level to 50 Pa, and let them stand for 24 h. (2) Place the group B unsealed wide mouth flasks in the vacuum drying oven, set the temperature to 30 °C and the vacuum level to 50 Pa, and let them stand for 16 h. (3) Place the group C unsealed wide mouth flasks into the temperature humidity chamber, set the temperature to 40 °C and the relative humidity to 30%, and let them stand for 48 h. (4) Place the group D unsealed wide mouth flasks in the laboratory under normal temperature and pressure and without treatment.

After the above processing, quickly add 230 mL dehydrated and degassed #25 insulating oil into 28 wide mouth flasks, respectively. Next, seal the wide mouth flasks, place them into the vacuum drying oven again, set the temperature to 40 °C and the vacuum level to 50 Pa, and let them stand for 24 h. At the end of this processing, put 24 flasks into six aging tanks. Each tank contains four samples with different moisture contents. The samples in the remaining four flasks are used to measure the initial parameters, which are shown in the Table 2. The six aging tanks are sealed and filled with nitrogen under atmospheric pressure, and placed in the accelerated aging box to undergo thermal aging 43 days at 130 °C.

Table 2. The initial parameters of test samples.

Group	A	B	C	D
Initial average moisture content/%	1.125	3.116	5.093	7.263
DP	1159	1173	1171	1165

2.3. The Measurement of Aging Characteristic Parameters

The Cartesian Coulomb moisture meter KF-831+KF-855 is used to measure the moisture content of the oil paper. The concept 80 testing system manufactured by Novocontrol Company is used to measure broadband dielectric spectroscopy. The testing frequency range of the system is from 10^{-6} Hz to 10^{5} Hz. The measurable parameters include the dielectric dissipation factor, the permittivity, the capacitance, the conductivity and so on. The NCY2 automatic viscosity tester manufactured by Shanghai Scientific Instruments Company is used to test the polymerization degree of the insulation paper, according to the relevant national standards referenced by "ASTMD 4243" [5].

3. Effect of Moisture on the Physical and Chemical Properties of the Insulating Paper

3.1. Change Trend of the Moisture Content in Insulating Paper

In the transformer oil paper insulation system, the moisture absorption ability of insulation paper is approximately 10^{4} times stronger than that of insulating oil, and the vast majority of moisture exists in the insulation paper when the moisture is in balance in the oil-paper insulation system [16]. For condenser bushing, the thickness of insulation paper is thinner than that of insulation paper in transformers and the moisture absorption ability is stronger, so the moisture is almost completely concentrated in the insulation paper, accelerating the insulation aging.

Figure 4 represents the moisture change rule of the insulation paper with different initial moisture contents during the aging process. The moisture content in the samples is found to show a decline in volatility during the aging process—the higher the initial moisture content, the greater the moisture fluctuation amplitude during the aging process. The moisture contents of group A, B and C reach lower levels after 15 to 20 days of aging—1.9% in group A, 2.3% in group B, and 2.1% in group C, whereas the moisture content of group D reaches 2.5%, a lower level after 30 days of aging. During the whole

aging process, the moisture contents of all four groups have different fluctuation amplitude—1.211% in group A, 1.691% in group B, 2.957% in group C, and 4.69% in group D. The moisture change rule of test samples is in accordance with that of oil-paper in transformers—that is, the more initial moisture there is, the greater is the moisture fluctuation amplitude in the paper [17,18].

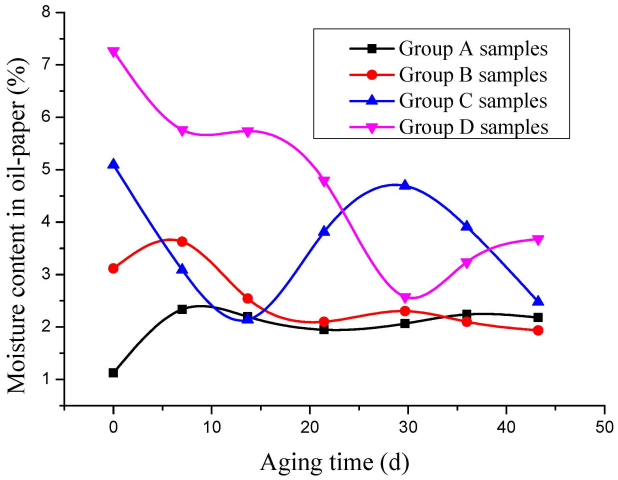

Figure 4. The moisture change rule of test samples.

The moisture contents of groups A and B both slightly increased and then decreased. The explanation for this phenomenon is as follows: the moisture absorbing capacity of insulation paper is very strong and the initial moisture content is at a low level and an unsaturated state, making it inevitable to absorb moisture from the air during the process of operation. Thereby, the moisture content slightly increased during the initial aging period. However, due to the positive feedback of aging byproducts, the consumption rate of moisture will be accelerated. In addition, the moisture may be transferred to oil with an increase of temperature, leading to the decrease of moisture content in insulation paper [19]. Then, the absorption of moisture, the consumption of moisture and the transfer of moisture are in dynamic equilibrium, so large moisture fluctuation amplitude will not appear in the oil-paper insulation system.

The initial moisture contents of group C and D are at a high level after the initial preparations. During the initial aging period, the moisture transfer from insulation paper to insulation oil, and the moisture in oil may be transferred to the air above the oil when the relative humidity of oil is greater than that of air. In addition, the hydrolysis of cellulose will consume moisture, thereby leading to the decrease of moisture content. However, the aging byproduct of insulation paper (acid) will accelerate the aging rate of insulating paper, producing more hydrophilic groups and hydrophilic impurities. The hydrophilic groups and impurities will adsorb more moisture, thereby leading to the increase of moisture content during the later aging period. It is because of the high initial moisture content in insulation paper, which leads to more serious aging and a larger amount of transferred moisture. Therefore, it needs more time to reach dynamic equilibrium, and the moisture fluctuation amplitude is at high level.

Reference [18] researched the moisture change rule of insulation paper in the transformer oil-paper insulation system, undergoing thermal aging at 130 °C. The initial moisture contents of the transformer oil-paper were 1%, 3% and 5%, and the moisture fluctuation amplitude were 0.7%, 2.4% and 4.3%, respectively [20,21]. However, the moisture fluctuation amplitude of test samples were 1.211%, 1.691% and 2.957%, respectively. It is observed that the moisture fluctuation amplitude of test samples is less than that of transformer oil-paper, except the initial moisture content is 1%. The reason is that the ratio of oil and paper is high, the moisture absorbing capacity of insulating paper is much stronger than the insulating oil, and the moisture transfer degree is low. The initial moisture content of group A is the lowest, which is maintained at approximately 2% during the aging process. In addition, the moisture fluctuation amplitude is only 0.389% after 15 days of aging. This phenomenon can be explained as

follows: the moisture absorption capacity of tested insulation paper is very strong, which can absorb external moisture easily during the process of operation. The moisture content of test samples is not easily maintained at a low level.

The results show that the mass ratio of oil and paper has little impact on the moisture fluctuation pattern in oil-paper but has great impact on the moisture fluctuation amplitude. The moisture fluctuation amplitude can indirectly reflect the condition of humidified insulation in bushing: the large moisture fluctuation amplitude of insulation paper indicates that insulation failure may occur during actual operation. On the contrary, the moisture content of insulation paper is relatively stable during the aging process, which indicates that the condition of humidified insulation is not serious.

3.2. Polymerization Degree (DP) of the Insulating Paper and Insulation Aging Rate

The degree of polymerization of insulating paper is the most intuitive and reliable indicator that can characterize the insulating paper aging degree [21]. In general, the polymerization degree of new insulating paper is more than 1000, and the paper reaches the end of its life when the polymerization degree decreases to a value of 250 [22]. The relationship between the degree of insulation paper polymerization and the aging time is in accordance with the kinetic model [23]. The work presented here uses a zero-order model to study oil-paper in capacitive bushing formula (1):

$$\frac{1}{d_{DP_t}} - \frac{1}{d_{DP_0}} = kt \tag{1}$$

where t is the aging time, d_{DPt} is the degree of polymerization of the insulating paper at time t, d_{DP0} is the initial value of the degree of polymerization, and k is the average aging rate, representing the degradation rate of the insulation paper during the aging process.

The DP of the different groups decreases, as shown in Figure 5. Zero order kinetic model fitting is shown in Figure 6. The fitting results of the aging rate and goodness of fit are shown in Table 3. The results show that the higher the initial moisture content, the faster decline in DP of insulating paper in the aging process. This phenomenon can be explained by the hydrolysis of cellulose [24]. In addition, hydrogen bonds between the moisture and the insulation paper can reduce the number of hydrogen bonds between the cellulose chains, thus reducing the stability of the molecular chains and increasing the breaking of cellulose.

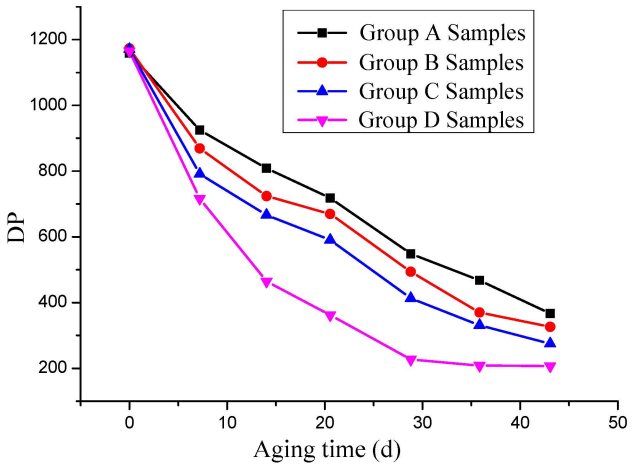

Figure 5. The DP change rule.

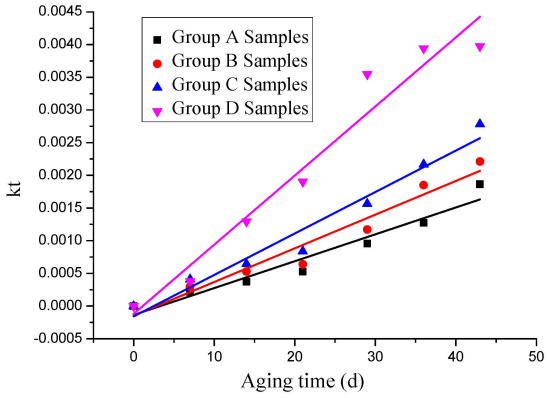

Figure 6. The zero-order dynamics model.

From Table 3, the decrease of insulating paper DP in this test sample is in accordance with the zero-order kinetic model. The aging rate k is between 2×10^{-5}–2.5×10^{-5} in the transformer oil-paper when the initial moisture content is 1% [25]. However, the aging rate of group A is about 4.1×10^{-5}, which is approximately twice as larger as that of paper in transformer when the initial moisture content of paper is 1%. This behavior can be explained as follows: the test paper is much thinner than that used in the transformer, the specific surface area of cellulose is larger, and the moisture absorption ability is stronger. These factors cause the rate of cellulose degradation to increase [25,26]. In addition, the ratio of oil and paper in the bushing model is far less than that in the transformer, and the initial moisture content of insulation paper is the mass ratio of moisture and paper. Thus, for the entire system insulation, the total moisture content in the unit volume sample is far greater than that in the transformer. Thus, small molecule substances such as water, acid, *etc.*, can be easily spread in the cellulose, which can lead to the high degradation rate of the paper.

Table 3. The average aging rate k and goodness of fit R^2.

Sample Group	Sample k	Transformer Oil-Paper k_1	Transformer Oil-Paper k_2	R^2
A	4.132×10^{-5}	2.29×10^{-5}	2.466×10^{-5}	0.9431
B	5.179×10^{-5}	7.42×10^{-5}	8.665×10^{-5}	0.9482
C	6.374×10^{-5}	8.62×10^{-5}	11.75×10^{-5}	0.9611
D	10.59×10^{-5}	—	—	0.9443

Meanwhile, with higher moisture content, the average aging rate of the test sample is lower than that of insulation paper in the transformer. This behavior can be explained as follows: the cellulose molecular chains are easier to fracture among long chains, so the low molecular weight cellulose is harder to fracture compared to the high molecular weight cellulose. Therefore, the decomposition of cellulose is rather intense during the initial aging period. However, the number of long cellulose molecular chains will decrease sharply during the later aging period, leading to the decrease of cellulose decomposition rate. Considering the average decomposition rate during the whole aging process, for the thinner insulation paper with high moisture content in bushing, the number of long cellulose molecular chains is less than that in the transformer, leading to the aging rate being smaller during the later aging period. Thus, the average aging rate of the test sample is lower than that of insulation paper in the transformer during the whole aging process.

From this section, it is clearly observed that bushings are vulnerable to moisture. This vulnerability plays an important role in the accelerated aging of the insulation. However, when applying the observations to onsite assessments, the measurement of DP is a destructive measurement and difficult to realize; as a result, researchers must determine other characteristic quantities that are practicable for bushing insulation onsite monitoring.

4. How Aging and Moisture Content Affect tan δ

4.1. How Aging and Moisture Content Affect tan δ

Dielectric dissipation factor (tan δ) is defined as, dielectric material applied by external voltage, the internal energy loss caused by dielectric conductance and dielectric polarization, which indicates the ratio of active current and reactive current; dielectric dissipation factor does not depend on the geometric structure of the dielectric material [27].

Figure 7 shows the relationships between tan δ and aging time for samples with different initial moisture contents. Analysis of these diagrams indicates the following: first, tan δ tends to increase with decreasing applied frequency; second, the tan δ curve has two "deceleration zone", which appear in the frequency bands of 10^0–10^2 Hz and 10^{-1}–10^{-3} Hz, and in the former middle frequency band, tan δ has a strong relationship with aging time; third, the tan δ curve of high initial moisture content samples has a larger fluctuation range in the "deceleration zone". This phenomenon can be interpreted by Equation (2).

$$\tan\delta = \frac{\varepsilon''}{\varepsilon'} \tag{2}$$

where ε' is the real part of the dielectric coefficient, and ε'' is the imaginary part of the dielectric coefficient. With a reduction in the applied frequency, interfacial polarization is fully developed, leading to increasing polarization loss and an increment of ε''. At the same time, ε' is increasing with the increase of the polarization intensity [28]. The complex correlations between polarization intensity and the speed of polarization result in the "deceleration zone" in a certain frequency band, which is determined by the measuring temperature, oil paper constituents, aging time, and moisture content [24,29].

Because the insulation structure of the capacitance core in the oil-paper bushing is relatively simple, the polarization of the oil-paper is weaker than that of the transformer oil-paper. In addition, the moisture content of the test sample is at a relatively high level, so there are only "deceleration zones" and no minimum point.

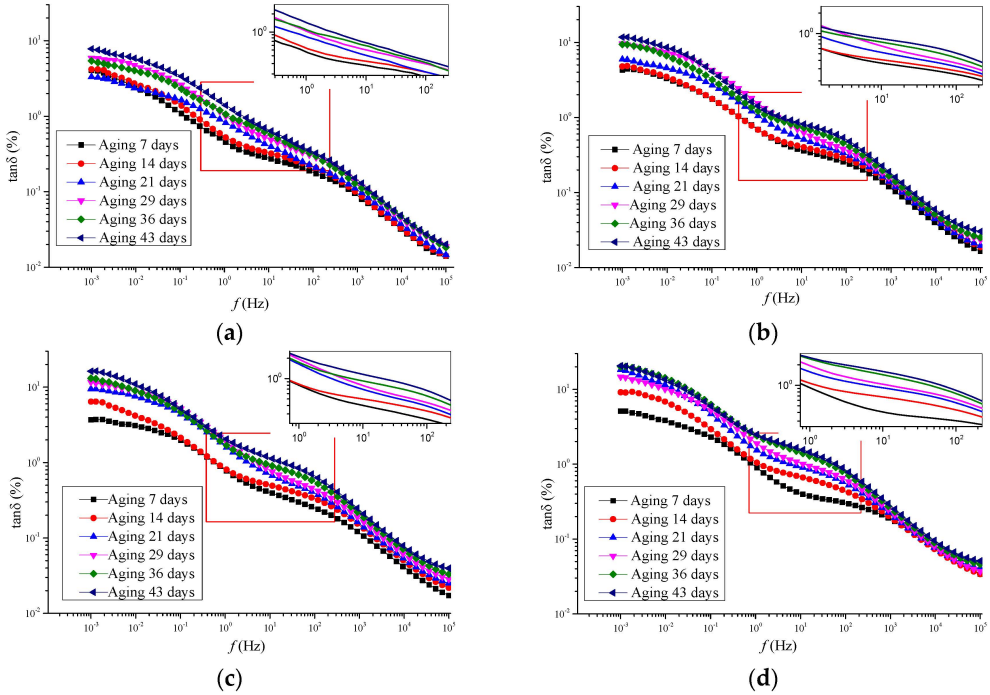

Figure 7. The tan δ curve change with frequency. (**a**) Samples in group A; (**b**) Samples in group B; (**c**) samples In group C; (**d**) samples in Group D.

4.2. Aging and Moisture Characteristics Based on tan δ

This investigation focuses on the integral value of tan δ in the characteristic interval, of which the range is 0.76828 Hz–234.26 Hz, and $I_{\tan\delta}(f)$ of samples with different moisture contents depends linearly on the aging time, as shown in Figure 8, Table 4 and Equation (3).

$$I_{\tan\delta}(f) = \int_{f_1}^{f_2} \tan\delta = A + Bt \tag{3}$$

where $I_{\tan\delta}(f)$ is equal to the integral value of tan δ in the characteristic interval and the characteristic interval is from f_1 to f_2, f_1 = 0.76828 Hz, f_2 = 234.26 Hz, t is the aging time, A is intercept and B is slope, which can be received by the fitting straight lines.

In addition, the analysis showed that $\Delta S_{I(\tan\delta)}$ and the initial moisture content in oil-paper apparently follow a linear law. As shown in Figure 9 and Equation (4).

$$\Delta S_{I(\tan\delta)} = P + Q \times (100m) \tag{4}$$

where $\Delta S_{I(\tan\delta)}$ is equal to the value of $I_{\tan\delta}(f)$ when aging 43 days minus the value of $I_{\tan\delta}(f)$ when aging seven days, m represents the moisture content of oil-paper, P and Q are not a certain values, which can be modified according to the actual situation.

From Table 4, the different initial moisture contents have an obvious influence on slope B, which represents the insulation aging rate characterized by the integral values of tan δ. The k_B represents the aging acceleration factor, the physical meaning of k_B is the increase degree of slope B with the increase of moisture. The value of k_{Bi} is equal to the insulation aging rate $B_{3\%}$, $B_{5\%}$ and $B_{7\%}$ divided by reference insulation aging rate $B_{1\%}$. The results of k_{Bi} are shown in Figure 10, the fitting curve accords with a cubic polynomial, and the goodness of fit is one.

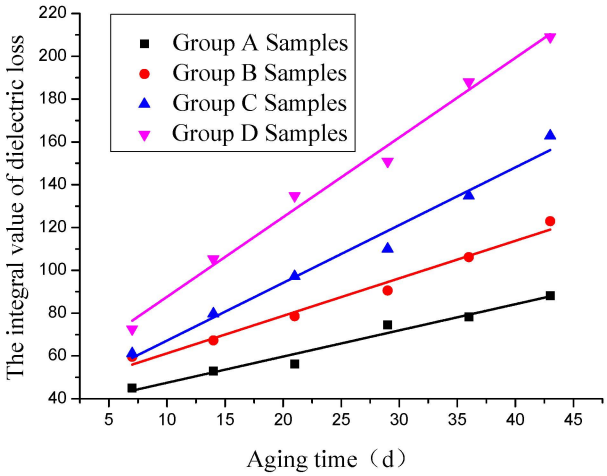

Figure 8. The fitting straight line between $I_{\tan\delta}(f)$ and aging time.

Table 4. The functional fitting parameters.

Parameters	Group A Samples	Group B Samples	Group C Samples	Group D Samples
Intercept A	35.25	43.69	40.20	50.39
Slope B	1.223	1.752	2.697	3.722
Goodness of fit R^2	0.9654	0.9785	0.9765	0.9872

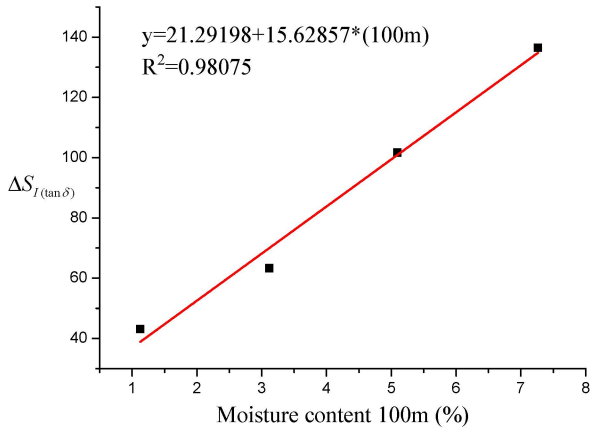

Figure 9. The fitting straight line between $\Delta S_{I(\tan\delta)}$ and moisture content.

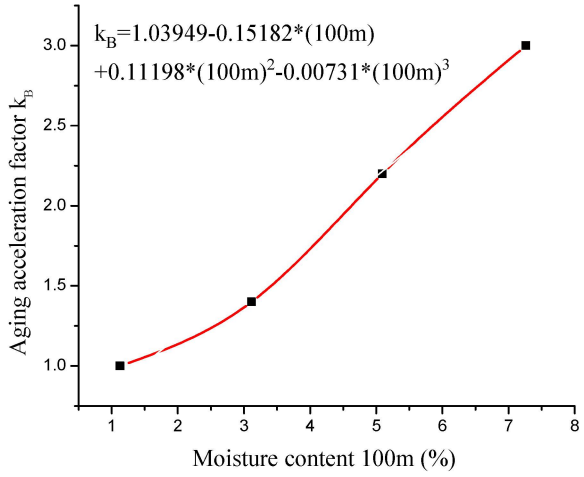

Figure 10. The fitting curve between k_B and moisture.

The life loss of insulation aging caused by damp conditions is calculated by imitating Arrhenius law, which is used to evaluate accelerated aging caused by temperature [28]. First, according to the integral value of the tan δ in the characteristic interval, the equivalent aging stage of the insulation can be calculated by Equation (5) (moisture is not considered for accelerated aging). Second, the damp state of the oil-paper bushing is evaluated by Equation (4), and the accelerated degree of insulation aging caused by the damp state is calculated using Equation (6). Next, the actual insulation aging state is calculated by Equation (7), and the average life of insulation is obtained by statistical data; as a result, the extent of the loss of insulation life can be determined for a device. F_{EQM} in Equation (6) is the equivalent accelerated aging factor calculated according to Figure 10.

$$t_{EQ} = \frac{I_{\tan\delta}(f) - A}{B} \tag{5}$$

$$F_{EQM} = \frac{\sum_{i=1}^{N} k_{Bi}\Delta t_i}{\sum_{i=1}^{N} \Delta t_i} \tag{6}$$

$$t_{loss} = \frac{F_{EQM} \times t_{EQ}}{L_p} \times 100 \tag{7}$$

In Equations (5)–(7), k_{Bi} is the aging acceleration factor caused by moisture at time t_i, Δt_i is the time period of insulation dampness, F_{EQM} is the equivalent accelerated aging factor caused by insulation dampness during the actual time t, t_{loss} is the loss ratio of insulation life (in units of %), t_{EQ} is the equivalent aging stage of insulation, and L_p is the statistics of the normal operating life of oil-paper bushing operating at the condition of normal temperature and dry condition, whose dimension should be consistent with t.

According to the evaluating method provided in this paper, the loss ratio of insulation life t_{loss} of test samples can be evaluated by the test data. The aging time t and DP_T (T is the end point of aging life of insulation paper) are set to 25 days and 250, respectively, and L_p is derived by formula (1), according to test data of samples in group A. The aging state parameters of test samples with different initial moisture contents are shown in Table 5.

Table 5. The state parameters of test samples.

Sample Group	A	B	C	D
k_{B1} (0~7 days)	1.000	1.433	2.205	3.043
k_{B2} (7~14 days)	1.203	1.612	1.423	2.484
k_{B3} (14~21 days)	1.168	1.257	1.155	2.473
k_{B4} (21~25 days)	1.114	1.147	1.683	2.080
F_{EQM}	1.122	1.388	1.609	2.573
L_p/days	76	76	76	76
t_{loss}/%	36.91%	45.66%	52.92%	84.63%

As shown in Table 5, the equivalent accelerated aging factor F_{EQM} and the loss ratio of insulation life t_{loss} have a positive relationship with the initial moisture content, which indicates that the initial moisture content has significant impact on the aging rate of insulation paper and the moisture accelerates the aging of insulation paper. The humidified condition of oil-paper condenser bushing can be quantitatively evaluated by the loss ratio of insulation life based on frequency domain dielectric spectroscopy.

The relationships between $I_{\tan\delta}(f)$ and aging time, $\Delta S_{I(\tan\delta)}$ and moisture content revealed that $I_{\tan\delta}(f)$ not only reflects the aging degree but also the moisture content in solid insulation. From another perspective, the frequency domain dielectric spectroscopy (FDS) results of oil-impregnated paper may be impacted by the moisture content and the aging time, simultaneously. Some separation attempts of moisture content and aging time have been reported recently, but it must be emphasized that moisture and aging separation still constitute a challenging point in this domain [11,30,31].

5. Conclusions

By designing the capacitor core models of condenser bushing with different initial moisture contents, carrying out a 43-day accelerated thermal aging test at 130 °C and studying the variation of the relevant parameters during the aging process, the following conclusions are drawn.

(1) The moisture fluctuation amplitude can reflect the different initial moisture contents of insulating paper; this result is in accordance with the conclusion of transformer oil-paper insulation that the higher the moisture content, the greater the moisture fluctuation amplitude. Furthermore, the moisture fluctuation amplitude of the tested oil-paper was lower than that of the oil-paper in transformer under the same initial moisture content. These results show that the mass ratio of oil and paper has little impact on the moisture content fluctuation pattern in oil-paper but has a great impact on moisture fluctuation amplitude.

(2) The DP of insulation paper in condenser bushing conforms to the zero-order kinetics model. Moreover, the aging rate of test oil-paper is higher than that of oil-paper in transformers under low moisture content but lower than that of oil-paper in transformers under high moisture content. These

results indicate that the initial moisture content has appreciable impact on the decline rate of the degree of polymerization during the initial aging period.

(3) Two obvious "deceleration zones" appeared in the dielectric spectrum with the decrease of frequency: 10^0-10^2 Hz and $10^{-1}-10^{-3}$ Hz. In addition, tan δ has strong regularity with the aging time in middle-frequency interval. Analysis revealed that $I_{\tan\delta}(f)$ and aging time, $\Delta S_{I(\tan\delta)}$ and moisture content both conform to linear rules. The behavior indicates that $I_{\tan\delta}(f)$ not only reflects the aging degree but also the moisture content in solid insulation. Consequently, the condition of humidified insulation and the aging state of solid insulation can be evaluated by analyzing $I_{\tan\delta}(f)$, and this investigation provides an idea to quantitatively evaluate the insulation condition of busing in the field.

Acknowledgments: The reported study was performed due to the Funds for Innovative Research Groups of China (51321063).

Author Contributions: The article was finished by a team, every author took part in the whole work. The design of the test and the extraction of parameters were provided by Binjun Chen. The analysis method of the impact of initial moisture content on oil impregnated paper was performed by Youyuan Wang. The processing of data was done by Yuanlong Li. Final review was done by Kun Xiao.

Conflicts of Interest: The authors declare no conflict of interest

References

1. Wang, S. Fault situation of transformer bushing and its analysis. *Transformer* **2002**, *39*, 35–40.
2. Li, H.L.; Hao, Y.L.; Zhong, L.; Li, L.; Shen, B.; Wang, M.; Han, L.G. Investigation on AC flashover of a 550 kV oil impregnated paper transformer bushing. *High Volt. Appar.* **2011**, *47*, 68–71.
3. Zhang, J.L.; Yan, J.; Guo, L. The case study of abnormal dielectric loss data of capacitive potential transformer bushings. *Shanxi Electr. Power* **2012**, *1*, 20–22. [CrossRef]
4. Zhang, X.Y.; Jiao, F.; Wang, W.K.; Wei, K.; Zhao, G. Development of oil-oil and Oil-SF6 resin impregnated paper capacitance graded transformer bushing. *Insul. Surg. Arresters* **2004**, *6*, 1–4.
5. Kes, M.; Christensen, B.E. Degradation of cellulosic insulation in power transformers: A SEC–MALLS study of artificially aged transformer papers. *Cellulose* **2013**, *20*, 2003–2011. [CrossRef]
6. Lundgaard, L.; Hansen, W.; Ingebrigtsen, S. Ageing of mineral oil impregnated cellulose by acid catalysis. *IEEE Trans. Dielectr. Electr. Insul.* **2008**, *15*, 540–546. [CrossRef]
7. Ingebrigtsen, S.; Dahlund, M.; Hansen, W.; Linhjell, D.; Lundgaard, L.E. Solubility of carboxylic acids in paper (Kraft)-oil insulation systems. In Proceedings of the 49th IEEE Electrical Insulation and Dielectric Phenomena, Boulder, CO, USA, 17–20 October 2004; pp. 253–257.
8. Setayeshmehr, A.; Fofana, I.; Eichler, C.; Akbari, A.; Borsi, H.; Gockenbach, E. Dielectric spectroscopic measurements on transformer oil-paper insulation under controlled laboratory conditions. *IEEE Trans. Dielectr. Electr. Insul.* **2008**, *15*, 1100–1111. [CrossRef]
9. Bouaicha, A.; Fofana, I.; Farzaneh, M.; Setayeshmehr, A.; Borsi, H.; Gockenbach, E. Dielectric spectroscopy techniques as quality control tool: A feasibility study. *IEEE Electr. Insul. Mag.* **2009**, *25*, 6–14. [CrossRef]
10. Zaengl, W.S. Applications of dielectric spectroscopy in time and frequency domain for HV power equipment. *IEEE Electr. Insul. Mag.* **2003**, *19*, 9–22. [CrossRef]
11. Hadjadj, Y.; Meghnefi, F.; Fofana, I.; Ezzaidi, H. On the feasibility of using poles computed from frequency domain spectroscopy to assess oil impregnated paper insulation conditions. *Energies* **2013**, *6*, 2204–2220. [CrossRef]
12. Fofana, I.; Borsi, H.; Gockenbach, E. Results on aging of cellulose paper under selective conditions. In Proceedings of the IEEE Electrical Insulation and Dielectric Phenomena, Kitchener, ON, Canada, 14–17 October 2001; pp. 205–208.
13. Yang, L.J. Investigation on properties and characteristics of oil-paper insulation in transformer during thermal degradation process. *Trans. China Electrotech. Soc.* **2009**, *24*, 27–33.
14. Emsley, A.; Xiao, X.; Heywood, R.; Ali, M. Degradation of celulosic insulation in power transformers. Part 3: Effects of oxygen and water on ageing in oil. *IEE Proc.-Sci. Meas. Tech.* **2000**, *147*, 115–119. [CrossRef]
15. García, B.; Burgos, J.C.; Alonso, M.; Sanz, J. A moisture-in-oil model for power transformer monitoring-Part II: Experimental verification. *IEEE Trans. Dielectr. Electr. Insul.* **2005**, *20*, 1423–1429.

16. Pradhan, M.K.; Ramu, T. On the estimation of elapsed life of oil-immersed power transformers. *IEEE Trans. Dielectr. Electr. Insul.* **2005**, *20*, 1962–1969. [CrossRef]
17. Liao, R.J.; Wang, K.; Yi, J.G. Influence of Initial moisture on thermal aging characteristics of oil-paper insulation. *High Volt. Eng.* **2012**, *5*, 1172–1178.
18. Saha, T.K. Review of modern diagnostic techniques for assessing insulation condition in aged transformers. *IEEE Trans. Dielectr. Electr. Insul.* **2003**, *10*, 903–917. [CrossRef]
19. Pradhan, M. Assessment of the status of insulation during thermal stress accelerated experiments on transformer prototypes. *IEEE Trans. Dielectr. Electr. Insul.* **2006**, *13*, 227–237. [CrossRef]
20. Bozzo, R.; Gemme, C.; Guastavino, F.; Cacciari, M.; Contin, A.; Montanari, G.C. Aging diagnosis of insulation systems by PD measurements. Extraction of partial discharge features in electrical treeing. *IEEE Trans. Dielectr. Electr. Insul.* **1998**, *5*, 118–124. [CrossRef]
21. Gafvert, U.; Adeen, L.; Tapper, M.; Jonsson, G.B. Dielectric spectroscopy in time and frequency domain applied to diagnostics of power transformers. In Proceedings of the 6th IEEE International Conference on Properties and Applications of Dielectric Materials, Xi'an, China, 21–26 June 2000; pp. 825–830.
22. Saha, T.K.; Purkait, P. Investigation of an expert system for the condition assessment of transformer insulation based on dielectric response measurements. *IEEE Trans. Power Deliv.* **2004**, *19*, 1127–1134. [CrossRef]
23. Linhjell, D.; Lundgaard, L.; Gafvert, U. Dielectric response of mineral oil impregnated cellulose and the impact of aging. *IEEE Trans. Dielectr. Electr. Insul.* **2007**, *14*, 156–169. [CrossRef]
24. Blennow, J.; Ekanayake, C.; Walczak, K.; Garcia, B.; Gubanski, S.M. Field experiences with measurements of dielectric response in frequency domain for power transformer diagnostics. *IEEE Trans. Power Deliv.* **2006**, *21*, 681–688. [CrossRef]
25. Paraskevas, C.D.; Vassiliou, P.; Dervos, C. Temperature dependent dielectric spectroscopy in frequency domain of high-voltage transformer oils compared to physicochemical results. *IEEE Trans. Dielectr. Electr. Insul.* **2006**, *13*, 539–546. [CrossRef]
26. Poovamma, P.; Sudhindra, A.; Mallikarjunappa, K.; Ahamad, T.R.A. Evaluation of transformer insulation by frequency domain technique. In Proceedings of the IEEE International Conference on Solid Dielectrics, Winchester, UK, 8–13 July 2007; pp. 681–684.
27. Saha, T.; Purkait, P. Understanding the impacts of moisture and thermal ageing on transformer's insulation by dielectric response and molecular weight measurements. *IEEE Trans. Dielectr. Electr. Insul.* **2008**, *15*, 568–582. [CrossRef]
28. Koch, M.; Prevost, T. Analysis of dielectric response measurements for condition assessment of oil-paper transformer insulation. *IEEE Trans. Dielectr. Electr. Insul.* **2012**, *19*, 1908–1915. [CrossRef]
29. Lundgaard, L.E.; Hansen, W.; Linhjell, D.; Painter, T.J. Aging of oil-impregnated paper in power transformers. *IEEE Trans. Power Deliv.* **2004**, *19*, 230–239. [CrossRef]
30. Betie, A.; Meghnefi, F.; Fofana, I.; Yeo, Z. Neural network approach to separate aging and moisture from the dielectric response of oil impregnated paper insulation. *IEEE Trans. Dielectr. Electr. Insul.* **2015**, *22*, 2176–2184. [CrossRef]
31. Yao, Z.T.; Saha, T.K. Separation of ageing and moisture impacts on transformer insulation degradation by polarization measurements. In Proceedings of the International Conference on Large High Voltage Electric System, Paris, France, 26–30 August 2002; Volume 15, pp. 1–7.